

Case Report

Lymphocytic thyroiditis with an oncocytic alteration in a laboratory beagle

Osamu Hashiguchi^{1*}, Kohji Tanaka², Yuko Yamaguchi¹, Moeko Aoki¹, Nobuaki Sato¹, Takuro Endo¹, Maoko Yamaguchi², and Tsubasa Saito¹

¹Pathology Division, Gotemba Laboratory, BoZo Research Center Inc., 1284 Kamado, Gotemba, Shizuoka 412-0039, Japan

²Pathology Division, Tsukuba Laboratory, BoZo Research Center Inc., 8 Okubo, Tsukuba, Ibaraki 300-2611, Japan

Abstract: Histopathological, immunohistochemical, and ultrastructural characteristics of lymphocytic thyroiditis in an untreated four-year-old male beagle were described. Histopathologically, the thyroid glands were composed of two distinct cell types: round to oval cells with eosinophilic granular cytoplasm (Type A), which is consistent with the features of oncocytic oxyphils, and larger round cells with amphophilic or pale cytoplasm (Type B). These cell types extensively and diffusely infiltrated with a mixture of lymphocytes and plasma cells, destroying the follicular structure. Immunohistochemistry revealed that Type A cells were positive for thyroglobulin and cytochrome C, and that Type B cells were positive for calcitonin, synaptophysin, and cytochrome C. These results indicate that Type A and B cells stem from follicular and C cells, respectively. Ultrastructural investigation showed that microfollicles and microvilli were evident in the cytoplasm and along the luminal surface of Type A cells. Thus, the lymphocytic thyroiditis observed in the beagle exhibited a morphology similar to that of Hashimoto thyroiditis in humans, particularly in view of an oncocytic alteration of follicular cells. (DOI: 10.1293/tox.2024-0073; *J Toxicol Pathol* 2025; 38: 177–182)

Key words: thyroiditis, Hashimoto disease, oxyphil cells, oncocytic alteration, dog disease

Hashimoto's thyroiditis (HT) in humans is an autoimmune disorder that ultimately leads to hypothyroidism, which is histopathologically characterized by extensive lymphoplasmacytic infiltration associated with germinal centers, atrophic follicles, and Hürthle cells (oncocytic cells)¹. Thyroid glands exhibit progressive functional failure due to the autoimmune destruction of follicles resulting from a breakdown of self-tolerance to thyroid autoantigens¹.

Lymphocytic thyroiditis (LT) in animal species is a specific entity of disease that occurs spontaneously and experimentally. Several studies have demonstrated anti-thyroglobulin autoantibodies in the systemic circulation and immunocomplex depositions at the basement membrane of the follicular cells of the thyroid glands, suggesting an underlying autoimmune mode of action for spontaneous LT in animals². LT can be induced by immunization with heterogeneous thyroglobulins in dogs, rats, rabbits, monkeys, hamsters, and horses^{2–7}. In beagles, LT is a common that histologically resembles HT^{4, 5, 8}; however, oncocytic alter-

ations in follicular cells have rarely been described. This communication presents the histopathological, immunohistochemical, and ultrastructural findings of LT accompanied by oncocytic follicular cells in beagle dogs.

All procedures employed in this study were approved by the Institutional Animal Care and Use Committee of the Bozo Research Center, Inc. to comply with the concept of Animal Welfare.

The present case was on a male TOYO beagle dog purchased from Kitayama Labes Co., Ltd. (Yamaguchi, Japan) at 5-month-old, and remained untreated until euthanized at the age of 4 years in an individual stainless-steel cage (900 mm width × 850 mm depth × 750 mm height, Shinetsu-kanaami Corporation, Niigata, Japan) placed in a climate-controlled animal room at 22 ± 4°C; relative humidity, 55 ± 25%; air ventilation, 13–15 times/h and a 12-h light/dark cycle. The animals were provided with commercially available pelleted chow (DS-A; Oriental Yeast Co., Ltd., Tokyo, Japan) at a daily dose of 300 g with free access to tap water. A ball (SHS Ball, Marshall Bioresources Japan Inc., Ibaraki, Japan) and a stainless-steel chain (on the market) were offered for environmental enrichment. The care and treatment of the animal adhered to the recommendations outlined in the Guide for the Care and Use of Laboratory Animals issued by the Japanese Association for Laboratory Animal Science and Standard Operating Procedures of the Bozo Research Center, Inc.

The animal was euthanized at the age of 4 years for the humane endpoints of anorexia in the prone position. A panel

Received: 24 August 2024, Accepted: 7 December 2024

Published online in J-STAGE: 30 December 2024

*Corresponding author: O Hashiguchi

(e-mail: Hashiguchi-osamu@bozo.co.jp)

©2025 The Japanese Society of Toxicologic Pathology

This is an open-access article distributed under the terms of the Creative Commons Attribution Non-Commercial No Derivatives



(by-nc-nd) License. (CC-BY-NC-ND 4.0: <https://creativecommons.org/licenses/by-nc-nd/4.0/>).

of hematology and biochemistry tests revealed decreases in RBC, HGB, and HCT and increases in T-Chol. Anemia and hypercholesterolemia are the likely signs of hypothyroidism. In particular, the cholesterol level was elevated over the last 1 year from 450 to 783 mg/dL, prior to euthanasia. Other hematological and biochemical changes were independent of thyroid function.

Following euthanasia, the animals were necropsied and organs, including the thyroid glands, were sampled, fixed in neutrally buffered 10% formalin, embedded in paraffin, sectioned, and stained with hematoxylin and eosin (HE) for histopathology. The thyroid sections were subjected to further evaluation with periodic acid-Schiff (PAS) reaction, periodic acid methenamine silver (PAM), Masson's trichrome (MT) staining, immunohistochemistry (IHC) using primary antibodies listed in Table 1 either by a Vectastain Elite ABC Kit (Vector Laboratories Inc., Burlingame, CA, USA) or an EnVision+ System-HRP Labelled Polymer Kit (Agilent Technologies, Santa Clara, CA, USA)⁹, and electron micros-

copy on a formalin-fixed tissue by a JEM-1400 transmission electron microscope (JEOL Ltd., Tokyo, Japan) at 80 kV in accordance with the method of Widéhn *et al*¹⁰.

No gross pathological findings were evident in the thyroid glands at necropsy, and the cause of morbidity was unclear. Histopathology revealed LT accompanied by oncocytic alterations in follicular cells. The thyroid glands were extensively and diffusely infiltrated with inflammatory cells, primarily lymphocytes and plasma cells (Fig. 1A, 1B). These lymphocytes were positive for CD3 and CD20, with the latter being predominant, indicating prominent B cell infiltration (Fig. 1C, 1D). MT staining revealed numerous collagen bundles crisscrossing the thyroid glands (Fig. 1E). The follicles were considerably destroyed by lymphocytic infiltration, leaving a few intact follicles lined with cuboidal and hypertrophic epithelial cells (Fig. 1F), and containing exfoliated epithelia and inflammatory cells in the lumen. The colloid was positive to PAS (Fig. 1G).

The affected thyroid glands contained clusters consist-

Table 1. Primary Antibodies Used for Immunohistochemistry

Antibody	Clonality (clone)	Host	Antigen retrieval	Source	Dilution
CD3	Poly	Rabbit	AC, CB	Agilent Technologies (Santa Clara, CA, USA)	Ready-to-use
CD20	Poly	Rabbit	-	Life Technologies (Carlsbad, CA, USA)	1:400
Thyroglobulin	Poly	Rabbit	AC, CB	Agilent Technologies (Santa Clara, CA, USA)	1:6000
Calcitonin	Poly	Rabbit	MW, CB	Abcam (Cambridge, UK)	Ready-to-use
Synaptophysin	Mono (DAK-SYNAP)	Mouse	AC, TRS	Agilent Technologies (Santa Clara, CA, USA)	1:500
Ki-67	Mono (MIB-1)	Mouse	MW, CB	Agilent Technologies (Santa Clara, CA, USA)	Ready-to-use
Cytochrome C	Mono (A-8)	Equine	AC, CB	Santa Cruz Biotechnology (Santa Cruz, CA, USA)	1:100

AC: autoclave, 121°C, 10 min; CB: citrate buffer (pH 6.0); MW: microwave, 90°C, 10 min; TRS: Target Retrieval Solution (pH 9.0, Agilent Technologies).

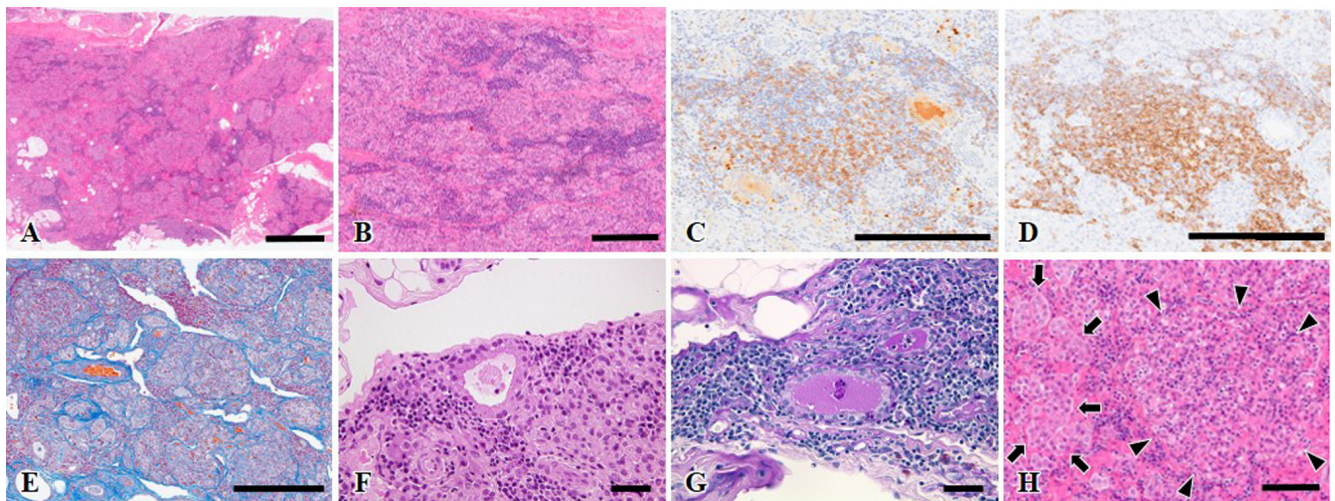


Fig. 1. Histopathological features of the thyroid glands in beagles. (A) The thyroid was replaced by eosinophilic cellular clusters, accompanied by lymphoplasmacytic infiltration. Few normal choroidal-filled follicles. HE. (B) Eosinophilic cellular clusters and lymphoplasmacytic infiltration. HE. (C) CD3-positive T cells. Immunostaining for CD3. (D) CD20-positive B cells. Immunostaining for CD20. (E) Abundant collagen bundles crisscrossing the thyroid gland. MT. (F) The remaining follicles are lined with cuboidal and hypertrophic epithelial cells. HE. (G) Colloids in the remaining follicles. PAS reaction. (H) Two cell types, Type A (arrowheads) and Type B (arrows). HE. Bars=1,000 μ m (A), 250 μ m (B, C, D, E), 100 μ m (H) and 50 μ m (F, G).

ing of two distinct cell types: round to oval cells with eosinophilic granular cytoplasm (Type A) and larger round cells with amphophilic or pale cytoplasm (Type B) (Figs. 1H, 2). Type A clusters comprise approximately 60% of all lesions. The IHC results are summarized in Table 2, and cells positive for each IHC marker are shown in Fig. 3. Both the cell types were randomly distributed across the thyroid gland (Fig. 4).

Type A clusters were composed of round to oval cells (Fig. 2A–2D). The cytoplasm was abundant, eosinophilic, and often granular with hyperchromatic nuclei and contained vacuoles that were positive for the PAS reaction (Fig. 2A, 2B). Each cell lacked polarity, gathered in the form of a densely compact cellular mass encircled by thick collagen bands and was subdivided into small nests of fine collagen fibers (Fig. 2C). The basement membrane formed around the compact cellular mass (Fig. 2D), and lymphoplasmacytic infiltration was prominent around and within the clusters. Type A cells were strongly positive for thyroglobulin (Fig. 3A) but negative for calcitonin or synaptophysin (Fig. 3E, 3I). These IHC results were consistent with the remaining intact follicles (Fig. 3C, 3G, and 3K), although

thyroglobulin staining was more intense in the present case than in healthy beagles (Fig. 3D).

Ultrastructural findings of Type A cells demonstrated microvilli along the luminal surface and small intracytoplasmic microfollicles that correlated with the vacuolation of HE sections. These are also the morphological characteristics of the follicular cells (Fig. 5A). Based on these findings, Type-A cells are thought to originate from follicular cells. A few cells positive for calcitonin and synaptophysin (Fig. 3E, 3I) in Type A clusters were considered C cells that were left unaffected. Notably, some Type A cells were strongly positive for cytochrome C, a well-known mitochondrial marker¹¹, indicating that abundant mitochondria were present in the cytoplasm (Fig. 3M). The follicular cells of the healthy beagles were negative for cytochrome C (Fig. 3P). Ultrastructural investigations failed to demonstrate mitochondria in Type A cells because of the poor quality of the samples.

Type B cells formed small nests that gathered to form large clusters (Fig. 2E–2H). The cytoplasm was pale or amphophilic (Fig. 2E). They were negative for PAS staining (Fig. 2F), and collagen fibers and basement membrane surrounded each nest (Fig. 2G and 2H). IHC revealed that

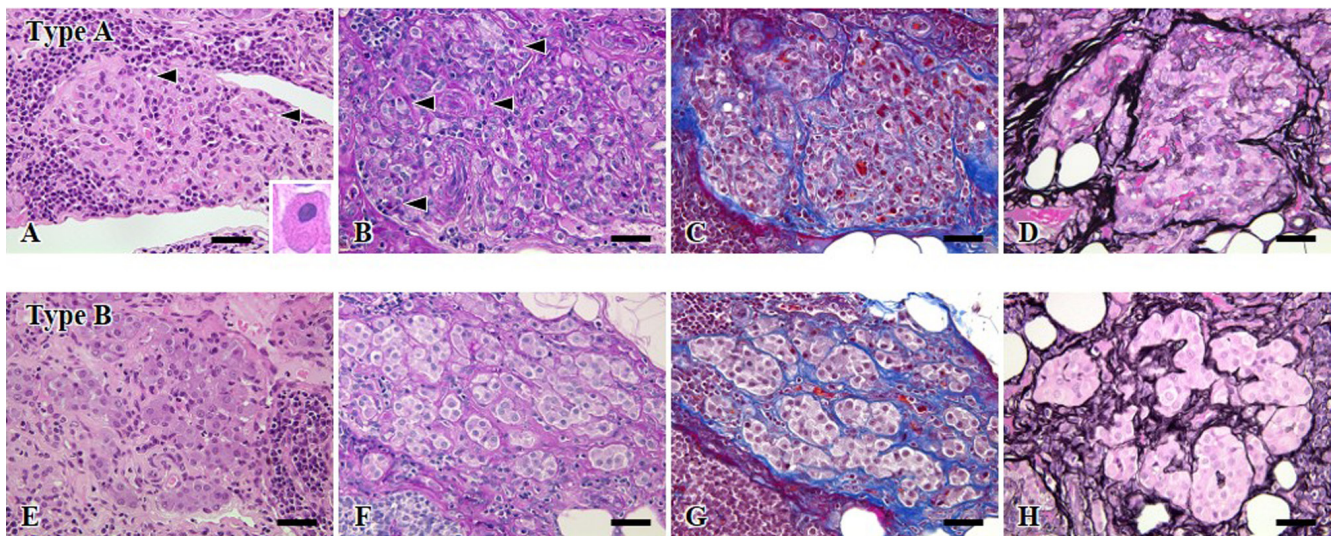


Fig. 2. Histopathological features of clusters of the two cell types in beagle dogs. Type A (A–D) and Type B (E–H) were stained with HE, PAS, MT, and PAM in order from the left. Type A cells had vacuoles (Fig. 4. A, arrowheads), and the vacuoles were positive for PAS staining (Fig. 4. B, arrowheads). Inset in photograph A: Eosinophilic granular cells with hyperchromatic nuclei. Bars=50 μ m.

Table 2. Immunohistochemical Reactivity of Each Thyroid Gland Component

Antibody	Type A	Type B	Remaining follicles	Corresponding normal thyroid of 1-year old male beagle dog
Thyroglobulin	++	-	+	+
Calcitonin	-*	++	-	++ (C-cells)
Synaptophysin	-*	++	-	++ (C-cells)
Ki-67	-	-	-	-
Cytochrome C	+ to ++	+	- to \pm	+

Positive intensity: -: negative; \pm : slightly; +: moderate; ++: strongly.

*A few positive cells judged remaining C-cells were present in the aggregation.

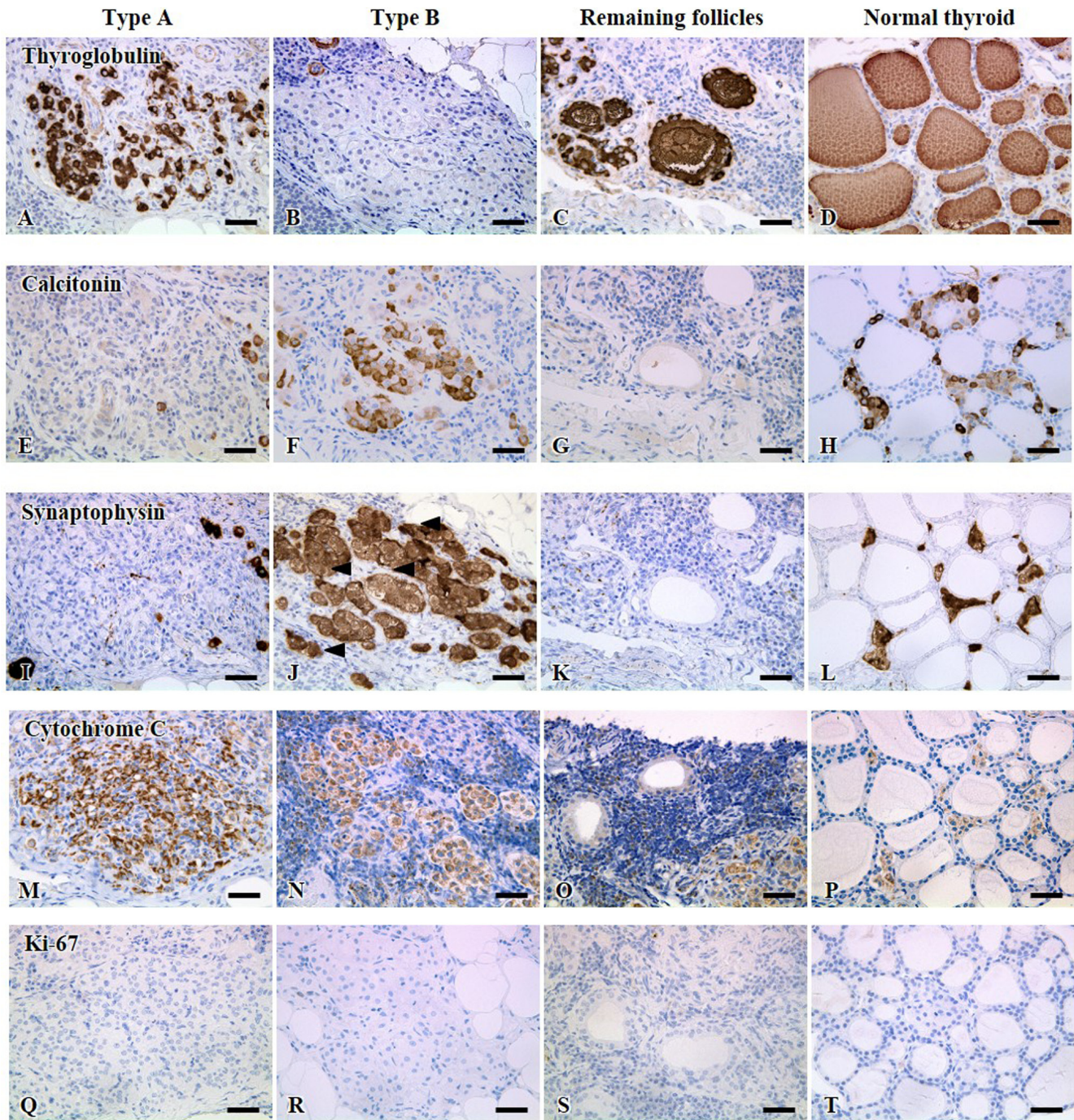


Fig. 3. Immunohistochemistry of thyroglobulin (A–D), calcitonin (E–H), synaptophysin (I–L), cytochrome C (M–P), and Ki-67 (Q–T) for Type A, Type B, remaining follicles, and a normal thyroid (a 1-year-old male beagle), respectively. Bars=50 μ m.

Type B cells were negative for thyroglobulin (Fig. 3B) and positive for calcitonin and synaptophysin (Figs. 3F, 3J), suggesting that they stemmed from C cells. This notion was supported by weakly positive staining for cytochrome C (Fig. 3N) and a number of secretory granules ranging from approximately to 100–200 nm in diameter, which is consistent with C-cells in beagle dogs on ultrastructural examination (Fig. 3P, Fig. 5B).

Proliferative potential was unlikely in both cell types

based on low positive indices of Ki-67, as in normal thyroid tissue (Fig. 3Q, 3R, 3T).

Persistent high serum levels of T-Chol, mild anemia, and atherosclerotic lesions in the arteries of several organs are sequelae of hypothyroidism in humans as a result of the inhibition of lipid metabolism and erythropoietin production¹. Similarly, a correlation exists between LT and hypothyroidism associated with subsequent symptoms in beagle dogs^{12–14}, and the clinical signs of hypothyroidism are pre-

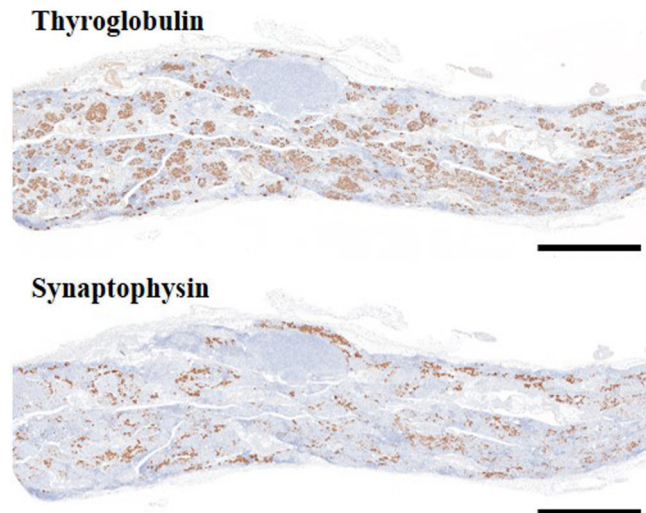


Fig. 4. Immunohistochemistry of thyroglobulin for Type A synaptophysin for Type B. Type A accounted for approximately 60% of lesions in all clusters. Bars=2 mm.

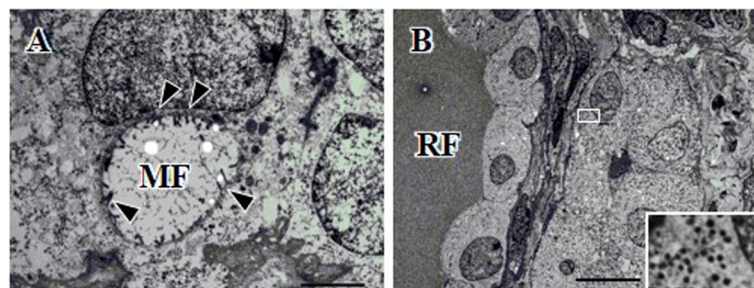


Fig. 5. Electron microscopy. (A) Intracytoplasmic microfollicles (MF) and microvilli (arrowheads) along the luminal surface in Type A. (B) No colloid droplets were reabsorbed in the epithelial cells of the remaining follicle (RF). The number of secretory granules in Type B cells was consistent with that in type C cells. The inset shows a high-magnification view of the secretory granules. Bars=2 μ m (A), 10 μ m (B).

ceded by a severe degree of LT¹². Longstanding and significant LT most likely led to the development of hypothyroidism in this case of beagle.

The thyroid glands were damaged by extensive lymphoplasmacytic infiltration, leading to fibrosis and destruction of normal architecture. Only a few follicles with hypertrophic epithelium and a small number of C cell clusters remained unaffected. These histological features are consistent with the findings reported for LT in dogs^{3, 4, 12}. Compact cellular regions of C-cells or admixtures of C- and follicular cells have been reported in beagles with LT and hypothyroidism¹² as was observed in Type B clusters in the present case, whereas an oncocyte follicular alteration noted in Type A clusters is likely infrequent in the LT of beagles. Oncocytes are recognized as one of four histological indicators of HT in humans. They include extensive infiltration of lymphocytes and plasma cells, often with germinal centers; destruction and atrophy of the follicular structure; interstitial fibrosis; oncocytes characterized by abundant eosinophilic and granular cytoplasm; and a large, hyperchromatic nucleus with prominent nucleoli^{1, 15, 16}. Based on morpho-

logical similarities and a positive reaction to cytochrome C, eosinophilic granular cells consisting of Type A clusters are considered to represent the human counterparts of oncocyte oxyphils.

However, the pathogenesis underlying oncocyte development remains unknown. MT and PAM staining indicated that the affected thyroid glands were compartmentalized into groups of cells by collagen fibers and/or basement membrane. Thus, oncocytes may develop through a process in which the thyroid follicles first collapse due to lymphocytic infiltration, degenerative and regenerative follicular cells come into close contact, and are encased by reactive proliferative collagen bundles or the basement membrane; finally, these cells transform into oncocytes mediated by a metaplastic response. Microfollicles demonstrated by electron microscopy in Type A cells are indicative of follicular cell in LT in dogs⁸. Enlarged follicular cells are thought to develop through a metaplastic response to injury, resulting from the accumulation of altered mitochondria¹.

Both Type A and B cells are unlikely to be neoplastic or preneoplastic based on the low Ki-67 positive index com-

parative to normal thyroid tissues, together with the fact that two distinct cell types comprise the lesion.

Only a few reports have described LT, developing eosinophilic granular cells in dogs⁸; however, neither immunohistochemical nor ultrastructural analyses have been conducted on these cells, and cell clusters consisting of altered follicular cells have not been recognized. The present report details the LT in a dog, elucidates the similarity between LT in dogs and HT in humans, and provides additional information on background lesions in dogs, thereby contributing to further research on thyroid disease in humans.

Disclosure of Potential Conflicts of Interest: The authors declare no conflicts of interest associated with this study.

Acknowledgments: We express our gratitude to Dr. Kunitoshi Mitsumori, a Professor Emeritus of Tokyo University of Agriculture and Technology, and Dr. Minoru Tsuchitani, an Advisor of the BoZo Research Center, for their valuable and critical review of this manuscript. We also extend our appreciation to Mrs. Tomomi Yoshimoto for her technical assistance in preparing histological specimens.

References

1. Anirban M. The endocrine system. In: Robbins and Cotran Pathologic Basis of Disease, 8th ed. Kumar R, Abbas A, DeLancey A and Malone E (eds). Saunders, Pennsylvania. 1111–1113. 2010.
2. Glen CT. Endocrine system. In: Monographs on Pathology of Laboratory Animals Sponsored by the International Life Sciences Institute, 1st ed. Jones TC, Mohr U and Hunt RD (eds). Springer-Verlag, Berlin. 212–214. 1983.
3. Sato J, Doi T, Wako Y, Hamamura M, Kanno T, Tsuchitani M, and Narama I. Histopathology of incidental findings in beagles used in toxicity studies. *J Toxicol Pathol.* **25**: 103–134. 2012. [[Medline](#)] [[CrossRef](#)]
4. La Pelre KM. Endocrine system. In: Pathologic Basis of Veterinary Disease, 5th ed. Zachary JF and McGavin MD (eds). 660–697. 2012.
5. Jones TC, Hunt RD, King NW (eds). Endocrine gland. In: Veterinary Pathology, 6th ed. Williams & Wilkins, Maryland. 1232–1241. 1997.
6. Doi T, Tomonari Y, Kawasako K, Yamada N, and Tsuchitani M. Lymphocytic adrenal medullitis and lymphocytic thyroiditis in a laboratory beagle dog. *J Vet Med Sci.* **79**: 255–257. 2017. [[Medline](#)] [[CrossRef](#)]
7. Vajner L, Vortel V, and Brejcha A. Lymphocytic thyroiditis in beagle dogs in a breeding colony: histological findings. *Vet Med (Praha).* **42**: 43–49. 1997. [[Medline](#)]
8. Gosselin SJ, Capen CC, and Martin SL. Histologic and ultrastructural evaluation of thyroid lesions associated with hypothyroidism in dogs. *Vet Pathol.* **18**: 299–309. 1981. [[Medline](#)] [[CrossRef](#)]
9. Moroki T, Matsuo S, Hatakeyama H, Hayashi S, Matsumoto I, Suzuki S, Kotera T, Kumagai K, and Ozaki K. Databases for technical aspects of immunohistochemistry: 2021 update. *J Toxicol Pathol.* **34**: 161–180. 2021. [[Medline](#)] [[CrossRef](#)]
10. Widéhn S, and Kindblom LG. A rapid and simple method for electron microscopy of paraffin-embedded tissue. *Ultrastruct Pathol.* **12**: 131–136. 1988. [[Medline](#)] [[CrossRef](#)]
11. Okawauchi M, Tsuboi M, Nibe K, Nagamine E, Iwane H, and Uchida K. Iridociliary adenocarcinoma with oncocytic change in a dog. *J Vet Med Sci.* **78**: 883–887. 2016. [[Medline](#)] [[CrossRef](#)]
12. Benjamin SA, Stephens LC, Hamilton BF, Saunders WJ, Lee AC, Angleton GM, and Mallinckrodt CH. Associations between lymphocytic thyroiditis, hypothyroidism, and thyroid neoplasia in beagles. *Vet Pathol.* **33**: 486–494. 1996. [[Medline](#)] [[CrossRef](#)]
13. Manning PJ. Thyroid gland and arterial lesions of Beagles with familial hypothyroidism and hyperlipoproteinemia. *Am J Vet Res.* **40**: 820–828. 1979. [[Medline](#)]
14. Jones TC, Hunt RD, King NW (eds). Cardiovascular system. In: Veterinary Pathology, 6th ed. Williams & Wilkins, Maryland. 997–998. 1997.
15. Asa SL, and Mete O. Oncocytic change in thyroid pathology. *Front Endocrinol (Lausanne).* **12**: 678119. 2021. [[Medline](#)] [[CrossRef](#)]
16. Dar RA, Chowdri NA, Parray FQ, and Wani SH. An unusual case of Hashimoto's thyroiditis with four lobed thyroid gland. *N Am J Med Sci.* **4**: 151–153. 2012. [[Medline](#)] [[CrossRef](#)]